

Massimiliano Gei

Dipartimento di Scienze e Metodi
dell'Ingegneria,
Università di Modena e Reggio Emilia,
Via Fogliani 1, I-42100 Reggio Emilia, Italia
e-mail: mgei@unimo.it

Francesco Genna

Dipartimento di Ingegneria Civile,
Università di Brescia,
Via Branze 38, I-25123 Brescia, Italia
e-mail: genna@bscivgen.ing.unibs.it

Davide Bigoni

Dipartimento di Ingegneria
Meccanica e Strutturale,
Università di Trento,
Via Mesiano 77, I-38050 Trento, Italia
e-mail: bigoni@ing.unitn.it

An Interface Model for the Periodontal Ligament

A nonlinear interface constitutive law is formulated for modeling the mechanical behavior of the periodontal ligament. This gives an accurate interpolation of the few available experimental results and provides a reasonably simple model for mechanical applications. The model is analyzed from the viewpoints of both mathematical consistency and effectiveness in numerical calculations. In order to demonstrate the latter, suitable two- and three-dimensional nonlinear interface finite elements have been implemented.

[DOI: 10.1115/1.1502664]

1 Introduction

The presence, in the jaw bone-teeth system, of a very thin interface made of soft tissue—the periodontal ligament (hereafter abbreviated as PDL)—strongly influences the stress state of such a system and poses significant difficulties in its mechanical modeling. In particular, two main problems can be easily pinpointed: (i) the existence of very different length scales (that of the jaw-teeth system and that of the PDL and its internal constituents); (ii) the so far scarcely explored, very complex mechanical behavior of the PDL. Indeed, in most numerical analyses the PDL is modeled as a homogeneous, linearly elastic continuum (McGuinness et al. [1]; Middleton et al. [2]; Rees and Jacobsen [3]; see also Moxham and Berkovitz [4] for a qualitative analysis of the PDL behavior) and a similar problem setting has been also assumed in the analysis of dental implants including a soft stress absorbing/redistributing layer, somehow emulating the PDL (van Rossen et al. [5]).

An accurate stress analysis of the teeth-PDL-bone system appears as a basic step in a correct understanding of its complex mechanical-biological behavior, with implications also in the design of effective and reliable fixed dental implants (see Brunski [6] for a review of this particular field). In the present work we attack the above-mentioned difficulties in a purely mechanical perspective, through the proposal of a mechanical model for the PDL. The latter provides the basis for an effective Finite Element technique, potentially useful to obtain accurate information about the stress and strain fields which develop, under loading, in the teeth-PDL-bone system. We start therefore from the few experimental results available in terms of the mechanical behavior of PDL (Ralph [7]; Pini [8]; Pini et al. [9]), which indicate that the PDL can hardly be treated as linear elastic. This suggestion is indirectly confirmed by the difficulties encountered by several authors in choosing a constant elastic modulus for the PDL; for instance, a variation of the Young modulus from 0.07 to 1750 MPa is reported in [3], a clear indication of the inadequacy of the linear elasticity assumption.

The experiments reported in [7–9] show that the PDL exhibits a monotonic stress-strain behavior analogous to that of many soft tissues (Fung [10]), with an early stage of extremely small stiffness followed, in higher deformation regimes, by a marked locking, i.e., a rapid increase of stress associated with a small increase of strain. The numerical treatment of such a nonlinear behavior in a

continuum framework, such as attempted, for instance, in [8,11–13], poses significant difficulties. In the first place, a large strain formulation is required; moreover, in terms of a Finite Element technique, a continuum discretization of the PDL requires indeed a fine, three-dimensional mesh, owing to the small thickness of the PDL itself. On the other hand, a “coarse” mesh is sufficient for describing bone and teeth. The necessary smooth transition between the characteristic lengths of the two meshes implies the use of an unnecessary large number of finite elements.

Here we propose an alternative approach, which allows one to avoid all the above-mentioned drawbacks. The key idea is to model the PDL as a nonlinear *interface*. In this way the PDL does not represent a third material subjected to large strains, as inevitable in a continuum description, and the analysis of the jaw bone-teeth system can be performed under the small-strain assumption. Modeling a thin layer of material as an interface is a well-established, successful concept in mechanics (Goland and Reissner [14]; Jones and Whittier [15]), which has recently received much attention (see e.g., Klarbring [16] and references cited therein).

Starting from the few available experimental results [7–9], we introduce a new interface constitutive model, able to phenomenologically reproduce the essential features of the observed experimental behavior. In such a way we obtain a reasonably simple tool which, introduced into a finite element code, enables us to describe in global terms the effects of the complex, nonlinear behavior of the PDL on the stress and strain states in the surrounding teeth and bone.

Our main purpose is methodological; no attempt is made here at obtaining results valid in an absolute sense for the human jaw bone-PDL-teeth system. We feel that even if the results given by the proposed model cannot be judged as absolutely accurate (at the present stage of the knowledge, it would be impossible to state what are the “exact” results for this problem), our model should represent a starting point and, more specifically, it might enable the analyst to obtain stress and strain states closer to “reality” than those computed so far. This feeling is justified by the fact that we have formulated and employed a model closer to the experimental evidence than those adopted so far; it is also confirmed by the indirect verifications, in terms of both tooth mobility and load-displacement curve for tooth extraction, that will be presented in Section 4. The availability of more accurate stress values, even if only in a relative sense, should constitute a better starting point for subsequent biological/physiological considerations, not addressed here.

The presentation will be limited to the instantaneous response

Contributed by the Bioengineering Division for publication in the JOURNAL OF BIOMECHANICAL ENGINEERING. Manuscript received April 2001; revised manuscript received June 2002. Associate Editor: L. J. Soslowsky.

of a tooth under the normal masticatory loading, under monotonic loading conditions only, so that long-term loads, such as orthodontic ones, are not addressed. This assumption allows us to treat both teeth and bone as simply isotropic linear elastic and to concentrate our attention simply to the nonlinearity introduced by the presence of the PDL.

2 The Mechanical Model

Two continuous bodies are considered, defined by the regions Ω^A and Ω^B in the Euclidean three-dimensional space, interacting with each other through a (sufficiently smooth) contact zone indicated by Ξ . At each point of the contact surface two unit normals may be defined, say \mathbf{n}^A and $\mathbf{n}^B (= -\mathbf{n}^A)$, directed away from Ω^A and from Ω^B respectively (Fig. 1). Small strains and displacements are assumed in the two bodies, characterized by a given constitutive law (assumed linear elastic in the applications) and subjected to the usual traction and/or displacement boundary conditions on their boundaries $\partial\Omega^A$ and $\partial\Omega^B$, except in the contact zone Ξ . In this region of the boundary a nonlinear interface constitutive law is prescribed in the way detailed below. Two essential requirements completely characterize the interface:

- the stress vector remains continuous across the interface, so that

$$\boldsymbol{\sigma}^B \mathbf{n}^B = -\boldsymbol{\sigma}^A \mathbf{n}^A, \quad (1)$$

where $\boldsymbol{\sigma}$ denotes the Cauchy stress tensor;

- the displacement may jump across the interface, but we assume a constitutive law relating the displacement jump to the stress vector. This may be generically written as

$$\boldsymbol{\sigma}^B \mathbf{n}^B = \mathbf{g}(\boldsymbol{\delta}, \mathbf{n}^B, \mathbf{s}^B, \mathbf{t}^B), \quad (2)$$

where $\mathbf{g}(\cdot)$ is a vector-valued function both of $\boldsymbol{\delta} = \mathbf{u}^A - \mathbf{u}^B$, the jump in displacement, and of the vector triad \mathbf{n}^B , \mathbf{s}^B , and \mathbf{t}^B , with unit vectors \mathbf{s}^B and \mathbf{t}^B defining the tangential plane to the interface.

The constitutive Eq. (2) must satisfy certain general mathematical requisites. In particular, with reference to the specific problem under study, we will assume:

1. isotropy of the response in the tangential plane, so that the function \mathbf{g} in (2) becomes a function of $\boldsymbol{\delta}$ and \mathbf{n}^B only:

$$\boldsymbol{\sigma}^B \mathbf{n}^B = \mathbf{g}(\boldsymbol{\delta}, \mathbf{n}^B); \quad (3)$$

2. invariance of \mathbf{g} under the full orthogonal group

$$\mathbf{Q}\mathbf{g}(\boldsymbol{\delta}, \mathbf{n}^B) = \mathbf{g}(\mathbf{Q}\boldsymbol{\delta}, \mathbf{Q}\mathbf{n}^B), \quad (4)$$

for every orthogonal tensor \mathbf{Q} , i.e., such that $\mathbf{Q}\mathbf{Q}^T = \mathbf{Q}^T\mathbf{Q} = \mathbf{I}$, \mathbf{I} indicating the identity tensor and superscript T the transposition operation;

3. existence of an interface potential ψ , such that

$$\mathbf{g}(\boldsymbol{\delta}, \mathbf{n}^B) = \frac{\partial \psi}{\partial \boldsymbol{\delta}}, \quad (5)$$

where ψ is a scalar-valued function of vectors $\boldsymbol{\delta}$ and \mathbf{n}^B . Condition (4) implies that ψ is an isotropic function, namely, that it satisfies $\psi(\boldsymbol{\delta}, \mathbf{n}^B) = \psi(\mathbf{Q}\boldsymbol{\delta}, \mathbf{Q}\mathbf{n}^B)$. As a consequence, the function ψ must depend only on the scalar product of $\boldsymbol{\delta}$ and \mathbf{n}^B and on the modulus of $\boldsymbol{\delta}$ (Truesdell and Noll [17]), so that

$$\psi = \psi(\delta_n, \delta_t), \quad (6)$$

where $\delta_n = \boldsymbol{\delta} \cdot \mathbf{n}^B$ and δ_t is the modulus of the vector $\boldsymbol{\delta}_t$, defined as

$$\boldsymbol{\delta}_t = \boldsymbol{\delta} - \delta_n \mathbf{n}^B. \quad (7)$$

In the absence of detailed experimental results, we have been guided by simplicity in assuming isotropy (3) in the tangential plane. Moreover, the existence of a potential (5) is consistent with the general laws of thermodynamics (and facilitates the numerical implementation). Finally, requisite (4) is related to the material frame indifference of the model [17].

Simple dimensional considerations show that the presence of an interface introduces a characteristic length in a mechanical problem [18]. Although not strictly necessary, we will identify this characteristic length with the thickness w_0 of the undeformed PDL.

The main objective of the next Section is the definition of a function $\mathbf{g}(\boldsymbol{\delta}, \mathbf{n}^B)$ which may properly model the mechanical behavior of the PDL. In what follows we will formulate a suitable nonlinear interface law for such a behavior, in which the normal interaction will be considered as uncoupled from the shear one. This assumption is guided by simplicity, owing to the lack of suitable experimental data.

This way of describing the PDL behavior allows us to confine all the nonlinearity into the interface, whereas the two surrounding bodies are treated in a fully linear way. Note also that we will always deal with monotonic loading of the interface and will not consider, therefore, any irreversible phenomena.

3 The Interface Law

3.1 Normal Interface Constitutive Law. Information regarding the mechanical behavior of the PDL under short-term loads can be deduced from the experimental results described in [8], which refer to uniaxial stress tests on bovine PDL specimens.

Stress-strain curves are reported in [8] using a second Piola-Kirchhoff uniaxial stress S versus uniaxial Green-Lagrange strain η representation. The Green-Lagrange strain may be written as

$$\eta = \frac{1}{2} \left(\frac{w^2}{w_0^2} - 1 \right) = \frac{\delta_n (\delta_n + 2w_0)}{2w_0^2} = \frac{\beta(\beta + 2)}{2}, \quad (8)$$

where w_0 and w are the thicknesses of the PDL in the undeformed and deformed state, respectively, and $\delta_n = w - w_0$. The dimensionless displacement jump parameter $\beta = \delta_n / w_0$ has been introduced to simplify the notation. The minimum value for η is -0.5 in compression, corresponding to $\delta_n = -w_0$ or $\beta = -1$, whereas in tension $\eta, \delta_n, \beta \in]0, +\infty[$.

In terms of experimentally measurable quantities, S can be written as

$$S = \frac{F w_0}{A_0 w}, \quad (9)$$

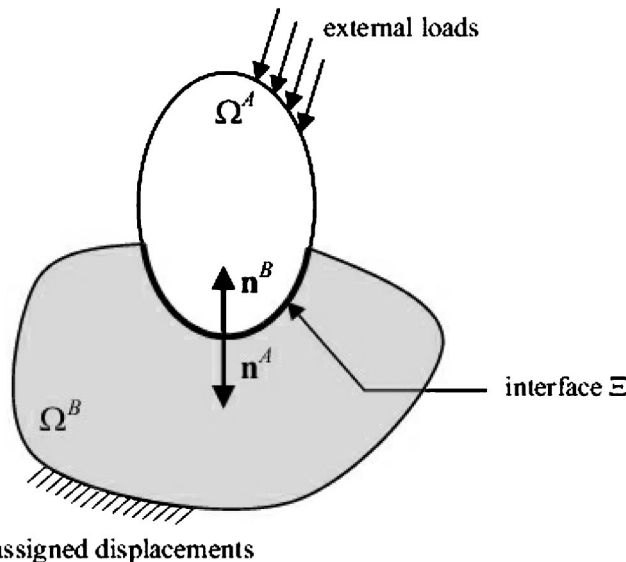


Fig. 1 Sketch of two continuous bodies in contact through the interface Ξ

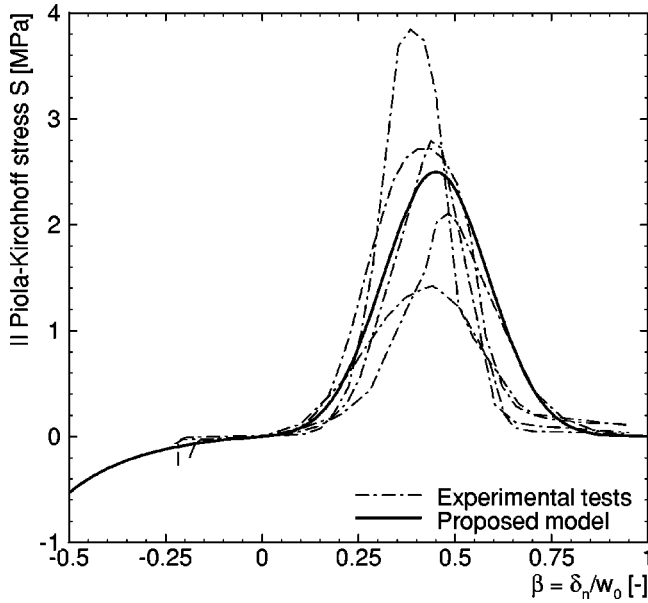


Fig. 2 Experimental [8] and proposed (Eqs. (10) and (11)) stress-strain curves for a uniaxial traction/compression test

where F is the total axial force which the specimen is subjected to, and A_0 is the area of its cross-section in the undeformed configuration.

In a (β, S) plot, typical experimental stress-strain data for bovine PDL, re-elaborated from [8], are reported in Fig. 2. To describe such experiments, we propose a normal interface constitutive law in the form

$$S = S_m f_n(\beta), \quad (10)$$

where S_m is the maximum stress reached in tension.

Our goal is to define the function $f_n(\beta)$, which provides the normal stress component once the displacement jump δ_n is prescribed across the interface. We propose the following function $f_n(\beta)$ both to fit a typical experimental result of [8] and to satisfy requisite (5):

$$f_n(\beta) = \begin{cases} b_1(e^{b_2\beta} - 1)e^{-b_3\beta^2}, & \beta \geq 0, \\ \frac{-b_4(e^{-b_5\beta} - 1)}{\beta + 1}, & -1 < \beta < 0, \end{cases} \quad (11)$$

where the non-dimensional coefficients b_i ($i = 1, \dots, 5$) are obtained by imposing the following five conditions:

$$\psi_n(\delta_n) = \begin{cases} -w_0 \frac{b_1 \sqrt{\pi}}{2\sqrt{b_3}} \left[\text{Erf}\left(\sqrt{b_3} \frac{\delta_n}{w_0}\right) + e^{b_2^2/4b_3} \text{Erf}\left(\frac{b_2 - 2b_3\delta_n/w_0}{2\sqrt{b_3}}\right) \right], & \delta_n \geq 0, \\ w_0 b_4 \left[-e^{b_5\delta_n/w_0} \text{Ei}\left(-b_5\left(1 + \frac{\delta_n}{w_0}\right)\right) + \ln\left(1 + \frac{\delta_n}{w_0}\right) \right], & -w_0 < \delta_n < 0, \end{cases} \quad (14)$$

In Eq. (14)

$$\text{Erf}(z) = \frac{2}{\sqrt{\pi}} \int_0^z e^{-x^2} dx, \quad \text{Ei}(z) = - \int_{-z}^{\infty} \frac{e^{-x}}{x} dx \quad (15)$$

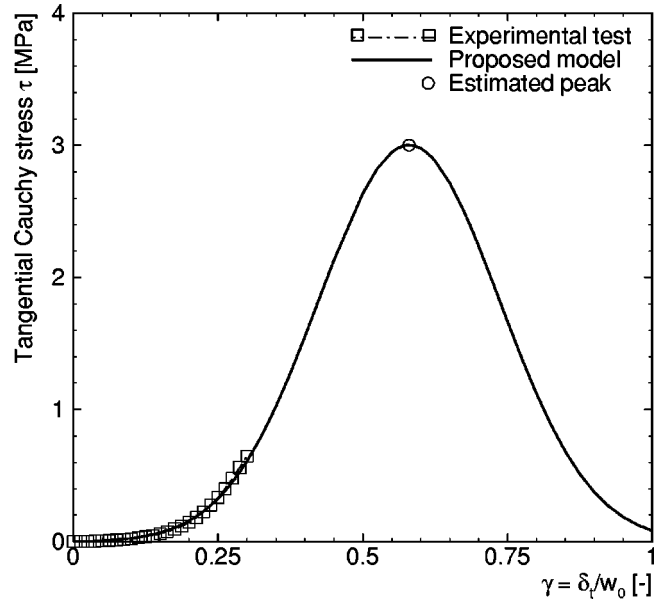


Fig. 3 Experimental [9] and proposed (Eqs. (17) and (18)) stress-strain curves for a shear test

$$f_n'(0^+) = f_n'(0^-) = E/S_m, \quad (\text{smoothness at } \beta=0),$$

where E is the slope of (10) at the origin;

$$f_n(\beta_m) = 1 \quad \text{and} \quad f_n'(\beta_m) = 0,$$

where β_m is the abscissa of the peak in tension;

$$f_n(\beta_c) = S_c/S_m,$$

where (β_c, S_c) is a representative point of the compression range of (10). Hence, coefficients b_i are functions of $E/S_m, \beta_m, \beta_c, S_c/S_m$. For instance, $b_1 b_2 = b_4 b_5 = E/S_m$.

By assuming $S_m = 2.5$ MPa, $E/S_m = 0.1$, $\beta_m = 0.45$, $\beta_c = -0.225$, $S_c/S_m = -0.04$, we obtain from the above five conditions

$$b_1 = 0.0041, \quad b_2 = 24.4395, \quad b_3 = 27.1555, \\ b_4 = 0.03694, \quad b_5 = 2.7071, \quad (12)$$

which define the solid curve of Fig. 2.

As desired, the function $f_n(\beta)$ admits a potential $\psi_n(\delta_n)$ such that

$$f_n(\beta) \equiv f_n\left(\frac{\delta_n}{w_0}\right) = \frac{d\psi_n}{d\delta_n}, \quad (13)$$

where

are the error function and the exponential integral function, respectively. As can be easily deduced from the curve of Fig. 2, the potential ψ_n is not convex.

3.2 Tangential Interface Constitutive Law. Recently published work [9] provides two experimental curves obtained from shear tests on bovine PDL specimens. These curves have been

interrupted much before the failure of the PDL (whereas the tension curves of [8] were given also for a post-peak regime); the adopted shear strain γ is

$$\gamma = \frac{\delta_t}{w_0}, \quad (16)$$

always non-negative. The experimental points that we have considered are shown in Fig. 3. In order to give a full stress-strain law, similar to that introduced for the normal behavior, we need to estimate the coordinates of the peak that would be present in Fig. 3, if the test were continued. This can be done—in an approximated way—on the basis of the previous results for uniaxial tension, as follows.

With reference to the value $S_m = 2.5$ MPa, the maximum uniaxial Cauchy stress is $\sigma_m = \lambda_m^2 S_m = 5.25$ MPa (having assumed an isochoric deformation, and using, for the stretch $\lambda = w/w_0$, the value at peak $\lambda_m = 1.45$). Adopting now the von Mises criterion of failure, the mean shear stress at failure in the uniaxial stress test is $\tau_m = \sigma_m / \sqrt{3}$, so that $\tau_m = 3.03$ MPa. Moreover, considering an infinitesimal cube rotated of $\pi/4$ with respect to the direction of stress, the shear strain at the peak is $\gamma_m \approx 0.58$. As a consequence, we estimate the peak in the shear stress/strain curve as $\gamma_m = 0.58$, $\tau_m = 3$ MPa.

With the above interpretation of the available experimental data, we proposed a shear stress-strain law of the form

$$\tau = S_m f_t(\gamma), \quad (17)$$

where the shape function $f_t(\gamma)$ is taken to be

$$f_t(\gamma) = c_1(e^{c_2\gamma} - 1)e^{-c_3\gamma^2}, \quad \gamma \geq 0. \quad (18)$$

Three conditions determine the non-dimensional coefficients c_i ($i = 1, 2, 3$):

$$f_t'(0) = G/S_m, \quad f_t(\gamma_m) = \tau_m/S_m, \quad f_t'(\gamma_m) = 0,$$

where G is the slope of (17) at the origin. Thus, the coefficients c_i may be expressed in terms of G/S_m , γ_m , and τ_m/S_m . The experimental results reported in Fig. 3 yield $G/S_m = 0.03$. The above three conditions define therefore the coefficients c_i as:

$$c_1 = 0.00127, \quad c_2 = 23.624, \quad c_3 = 20.366, \quad (19)$$

so that the analytical expression for the tangential constitutive law follows (represented by the solid curve in Fig. 3).

Again, as desired, the function $f_t(\gamma)$ admits a potential $\psi_t(\delta_t)$ such that

$$f_t(\gamma) \equiv f_t\left(\frac{\delta_t}{w_0}\right) = \frac{d\psi_t}{d\delta_t}, \quad (20)$$

where

$$\psi_t(\delta_t) = -w_0 \frac{d_1 \sqrt{\pi}}{2\sqrt{d_3}} \left[\text{Erf}\left(\sqrt{\frac{d_3}{w_0}} \delta_t\right) + e^{d_2^2/4d_3} \text{Erf}\left(\frac{d_2 - 2d_3\delta_t/w_0}{2\sqrt{d_3}}\right) \right]. \quad (21)$$

3.3 The Interface Constitutive Law. The general interface law (3) is now specified on the basis of the results obtained in the previous Subsections.

In terms of normal and tangential directions, Eq. (3) can be recast in the following form

$$\boldsymbol{\sigma}^B \mathbf{n}^B = g_n(\delta_n, \delta_t) \mathbf{n}^B + g_t(\delta_n, \delta_t) \mathbf{t}^B, \quad (22)$$

where $\mathbf{t}^B = \boldsymbol{\delta}_t / \delta_t$ and the functions $g_n(\delta_n, \delta_t)$ and $g_t(\delta_n, \delta_t)$ specify the interface behavior (i.e., the vector function \mathbf{g} of Eq. (3) has components g_n and g_t) and derive (see Eq. (5)) from a potential $\psi(\delta_n, \delta_t)$, so that

$$g_n(\delta_n, \delta_t) = \frac{\partial \psi}{\partial \delta_n}, \quad g_t(\delta_n, \delta_t) = \frac{\partial \psi}{\partial \delta_t}. \quad (23)$$

As already stated, we consider the normal and the shear behaviors of the PDL as uncoupled, assuming

$$\psi(\delta_n, \delta_t) = S_m [\psi_n(\delta_n) + \psi_t(\delta_t)], \quad (24)$$

where ψ_n is given by Eq. (14) and ψ_t by Eq. (21). As a consequence of Eqs. (23) and (24) we have

$$g_n(\delta_n) = S_m f_n(\beta), \quad g_t(\delta_t) = S_m f_t(\gamma), \quad (25)$$

where functions $f_n(\beta)$ and $f_t(\gamma)$ are given by Eqs. (11) and (18), respectively.

3.4 Uniqueness. Owing to the presence of non-convex terms in the potential functions $\psi_n(\delta_n)$ and $\psi_t(\delta_t)$, the solution of a boundary-value problem involving the interface law governed by Eq. (24) may be non-unique. This is a crucial point for the subsequent numerical investigations; its treatment is facilitated by the existence of a potential governing the adopted constitutive model. Here we give only the main results; the analytical details are reported, for the sake of completeness, in the Appendix.

The finite problem governed by the potential function defined by Eqs. (14, 21, 24) does not necessarily admit a unique solution, owing to the lack of convexity of the governing potential. However, in the numerical treatment of a quasi-static deformation path involving nonlinear effects, such as that introduced by our interface law (22), it is often necessary to refer to the so-called *incremental problem*. In such a problem, a generic equilibrium configuration of the system is supposed to be reached and the response to a small perturbation of the boundary data has to be found. The governing equations are thus expanded in a series of a time-like parameter controlling the deformation path, and, in the linear approximation, the first order terms are retained.

With the particular functions $f_n(\beta)$ and $f_t(\gamma)$ adopted here, a sufficient condition for the uniqueness of the solution of the *incremental* problem is that both the incremental normal $df_n/d\delta_n$ and tangential $df_t/d\delta_t$ stiffnesses of the interface are positive. With reference to Figs. 2 and 3, this corresponds to $\delta_n < 0.45w_0$ and $\delta_t < 0.58w_0$.

4 Numerical Results

The interface constitutive model described in the previous Sections has been implemented into a 6-node, 3 Gauss point interface

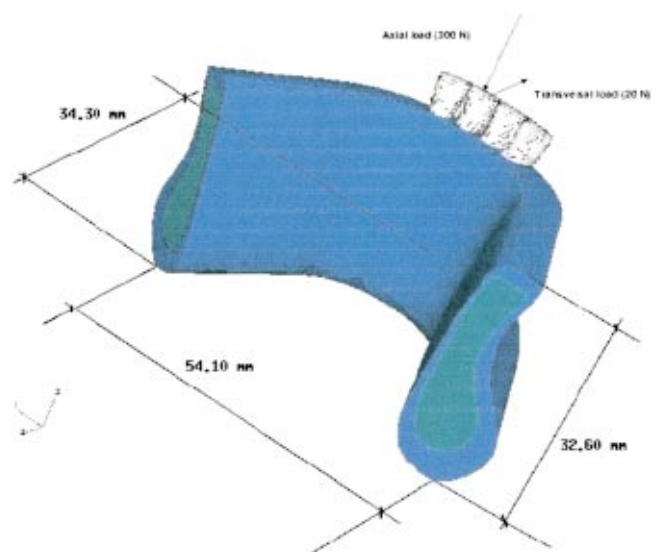


Fig. 4 Numerical model for the three-dimensional simulations. The model has 10092 nodes and 41996 elements, of which 37789 tetrahedral 4-noded elements and 4207 interface elements.

Table 1 Material properties used in the finite element analyses

Material	Young modulus E [MPa]	Poisson coefficient ν
Cortical bone	13700	0.3
Trabecular bone	1370	0.3
Dentine	20000	0.25
Enamel	80000	0.3

finite element, defined by two 3-noded triangles, each to be connected to a face of two adjacent 4-noded tetrahedral solid elements. To this purpose, we have exploited the UEL user subroutine, available in the Finite Element general-purpose code ABAQUS [19]. A suitable preprocessor has been coded to automatically insert interface elements, such as those implemented, into a pre-defined ABAQUS model.

Figure 4 illustrates the geometrical model considered for the Finite Element analyses, which allows one to distinguish between cortical and trabecular bone, and permits to account for the interaction between some adjacent teeth. The geometry has been constructed starting from an X-ray cross-section of a human jaw, extruded along a curved line roughly representing the middle axis of the mental portion of the jaw. This model has no special pretence to be exact from the anatomical viewpoint, but should anyway furnish reasonably accurate results in terms of mechanical quantities (see [20] for a discussion of the relevance of this type of Finite Element models in terms of stress analysis).

It is worth noting that we have also performed several two-dimensional stress analyses, not reported here for lack of space, of the tooth-PDL-bone system. In particular, we have implemented a standard 2-D version (plane stress/strain and axisymmetric) of the interface element, of the Goodman type [21]. Although on one hand we did obtain results showing the importance of taking into account the nonlinearity of the PDL, as found also adopting 3-D models, we found no quantitative agreement between the two and the three-dimensional results. We feel that this discrepancy should be emphasized, in view of the significant number of 2-D analyses of this problem found in the literature; this result con-

firms the findings by Corradi and Genna [20] and Meijer et al. [22], the latter with reference to the elastic analysis of fixed dental implants.

Coming back to the three-dimensional model of Fig. 4, fully fixed boundary conditions have been prescribed for simplicity at the lateral sides of the considered portion of the jaw; despite this further approximation, it is expected that the model provides results not sensibly different, in terms of stresses in the proximity of the tooth, from the situation relative to a full description of the jaw. Here we are only interested in the comparison between different assumptions, and for this purpose the geometry of Fig. 4 appears to be adequate [20].

The material data adopted for the linear elastic parts of the system are taken from [22] and summarized in Table 1.

We have investigated the effect of a purely axial load of 300 N, and of a purely transverse load of 20 N included in the sagittal plane and directed from the lingual to the labial side; these load values are among those suggested in the literature [6,23].

Our main purpose is to compare results obtained in the presence of the PDL modeled as an interface, treated either as illustrated in this paper or as a perfect interface (not allowing for displacement jumps, thus simulating the absence of the PDL), keeping fixed all the other model features and loading conditions. To this end, the map of the equivalent von Mises stress (a scalar measure of the global stress level defined as $\sqrt{3s \cdot s/2}$, s being the deviatoric part of the Cauchy stress tensor σ)¹ is reported in Figs. 5 to 8. In particular, Figs. 5 and 6 refer to the case of axial loading, whereas results obtained for the transverse loading are reported in Figs. 7 and 8; Figs. 5 and 7 pertain to the analyses in which the interface is perfect, whereas the results of analyses performed with the nonlinear PDL interface model are reported in Figs. 6 and 8. All the stress contours are in MPa units.

The comparison of the various results shows, in the first place, that the inclusion of a nonlinear interface into the model affects

¹Our choice of reporting only the von Mises stress is dictated by simplicity and conciseness. Obviously, our analyses give as a result all the mechanical quantities; the task of understanding which one of these interacts with the various biological functions in our problem falls beyond the scope of the present article.

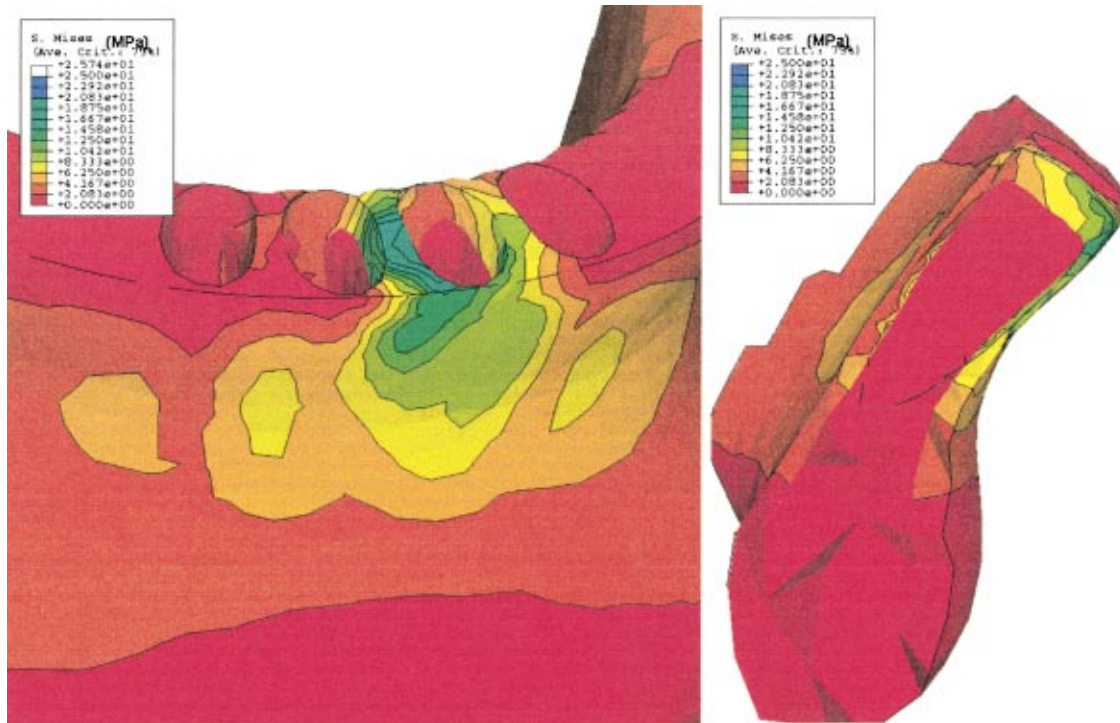


Fig. 5 von Mises equivalent stress: axial loading, PDL treated as a perfect interface

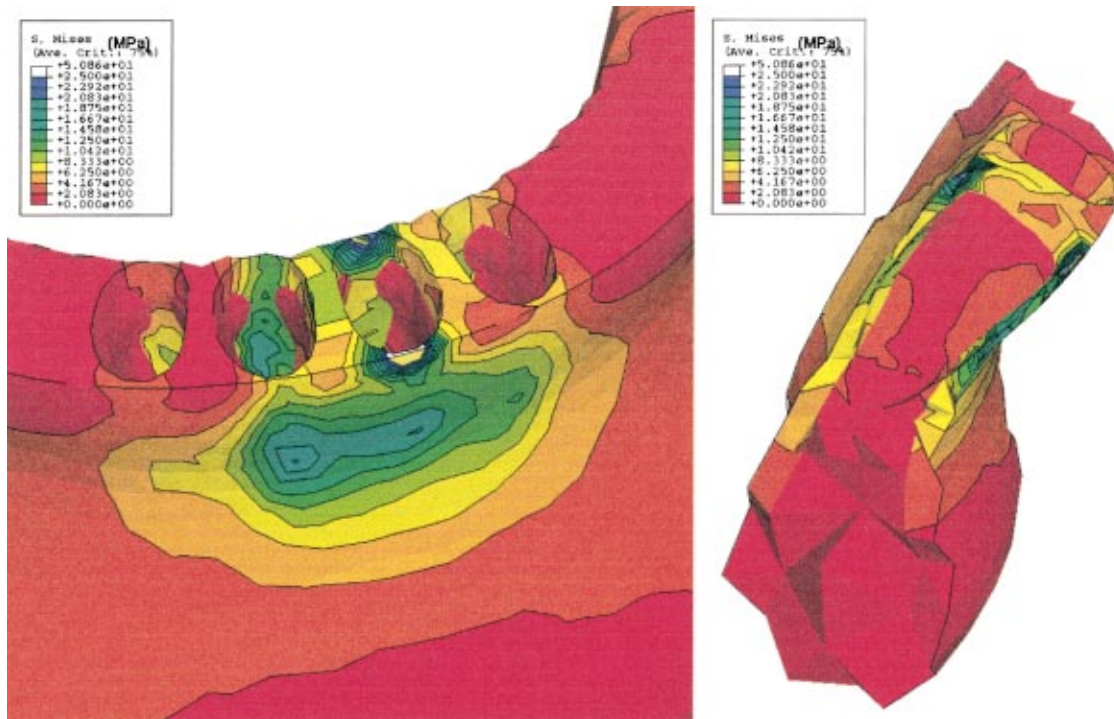


Fig. 6 von Mises equivalent stress: axial loading, PDL simulated by means of the proposed nonlinear interface element

qualitatively the stress state in the surrounding bone. In both loading cases the presence of the nonlinear PDL interface causes higher peak stresses than those existing in the perfect case; more interestingly, specially in the transverse loading case, the stress is much more diffused by the presence of the nonlinear PDL inter-

face, and the loading of a single tooth strongly influences the stress state around the surrounding teeth, which is not the case for the perfect interface.

The behavior computed in the case of a perfect PDL interface is also similar to that obtained treating the PDL as a linear interface.

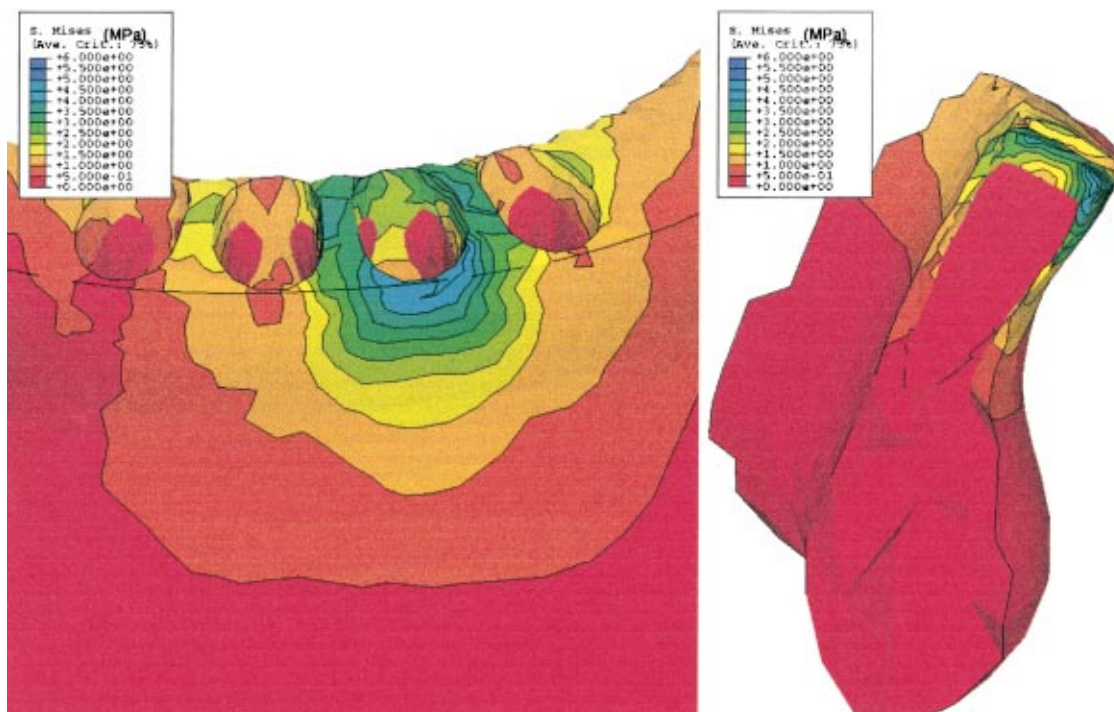


Fig. 7 von Mises equivalent stress: transverse loading, PDL treated as a perfect interface

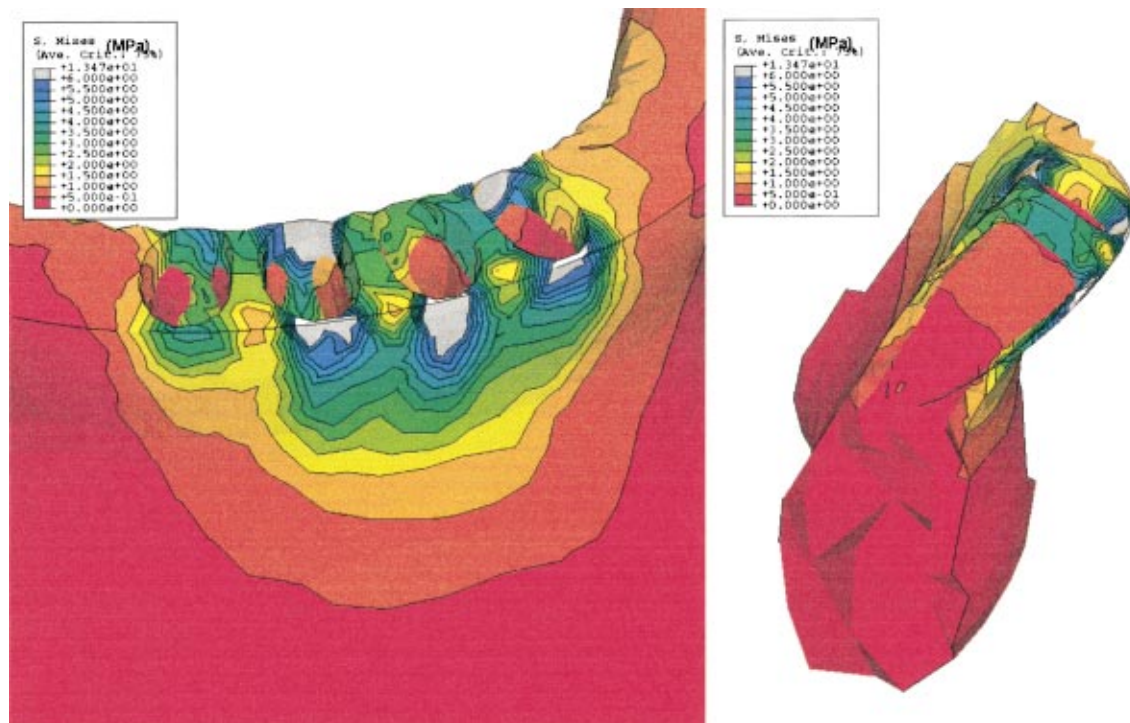


Fig. 8 von Mises equivalent stress: transverse loading, PDL simulated by means of the proposed nonlinear interface element

In such a case there is an obvious difficulty in identifying the stiffness of the interface, which, in reality, varies much, both in space and in time, as a function of the applied load and of the local stress distribution. We have used, as limiting cases, the initial and the maximum stiffnesses in tension given by our nonlinear interface model, i.e., $K_{L,min} = 1.25 \text{ MPa/mm}$, $K_{T,min} = 0.375 \text{ MPa/mm}$; $K_{L,max} = 55.9 \text{ MPa/mm}$, $K_{T,max} = 58.1 \text{ MPa/mm}$, K_L and K_T denoting longitudinal and tangential stiffnesses respectively, which relate tractions to displacement jumps. These values are also reasonable averages of those found experimentally in Pini [8]; note that in our calculations we have adopted the value $w_0 = 0.2 \text{ mm}$ for the interface thickness at rest.

There is no space here to fully report all the relevant results (some are shown in Fig. 9); it suffices to note that the use of constant values of the stiffnesses (constant both in space and in time) causes a significantly different stress distribution with respect to the nonlinear case, even if the peak stress values, for the high stiffness cases, are similar to the results of the nonlinear analyses (this could be expected, since the high load values adopted bring the nonlinear interface model to a regime of high stiffnesses). In particular, the strong stress redistribution predicted, under transverse loading, by the use of the nonlinear PDL model, is almost absent in the linear analyses, using both sets of values for the stiffnesses. It must also be added that while the nonlinear model takes into account implicitly the effect of contact in compression, the linear one, in the absence of explicitly defined contact surfaces, does not; therefore, when using low stiffnesses, for the high load values considered, compenetration occurs quite soon (at about 16 N for the vertical load and 6 N for the transverse load).

These results suggest that both the models of linear and perfect interfaces are not capable to predict important effects which are caught by the nonlinear ones. Even if it is impossible to directly conclude that these latter yield the “correct” results, owing to the impossibility of knowing the corresponding “exact” solutions in terms of local stresses, such a conclusion can be reached indirectly, by computing tooth mobility curves.

This can be done both in compression, a case in which experimental results are available, and in tension, to simulate the extraction process. Our results are compared in Fig. 9 with some experimental curves for tooth mobility in compression [6,7]. Two numerical results are included as obtained by the use of the linear interface as described above, whereas the third one, represented

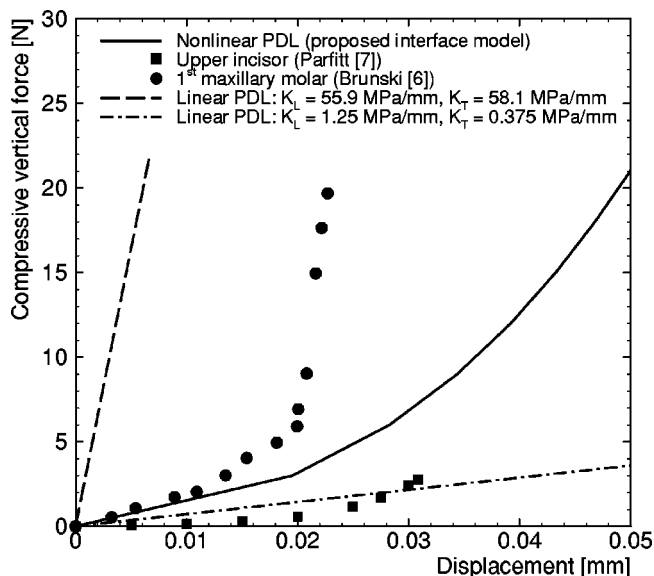


Fig. 9 Tooth mobility curves in compression: the symbols refer to experimental results for a molar [6] and an upper incisor [7], the lines to our simulations. The solid thick line has been obtained by using the proposed nonlinear interface model; the others by using linear interfaces as indicated.

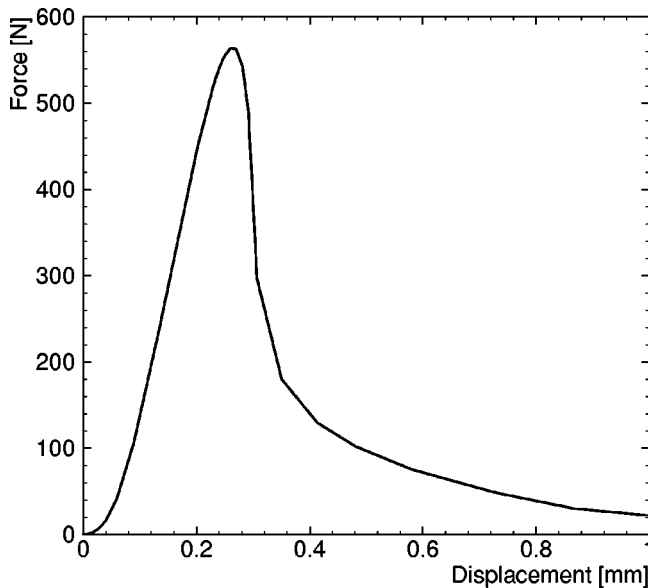


Fig. 10 Tensile axial load—axial displacement curve obtained from the numerical simulation of the extraction of the frontal incisor, mesh of Fig. 4

by the solid line, is given by the proposed nonlinear PDL model. Here the importance of taking into account the PDL nonlinearity becomes apparent.

As a final test, we have simulated the process of the extraction of a tooth, again using the mesh of Fig. 4 and applying a tensile axial load to the tooth to be extracted (no simulation of the real luxation process has been attempted). The relevant load displacement curve is shown in Fig. 10; special care must be exerted to obtain such a result numerically, since, after the peak load, the solution becomes unstable and is no more unique. In terms of validation of our model, we can first observe once more that the global aspect of the initial portion of the load-displacement curve is fully coherent with the known aspect of the mobility curves in compression, and note, further, that the peak load value, found at about 564 N, maybe high for a healthy human incisor, is definitely acceptable if we recall that we are using strength data, for the PDL, taken from tests on bovine teeth. Such a value is within the suggested range of forces necessary for the extraction of a tooth (100 to 800 N), and also the global aspect of the post-peak curve appears reasonable. The ability of obtaining such a result (impossible to find using a linear model) in a relatively simple way confirms the possibilities offered by the use of the proposed interface element within a three-dimensional context.

The cost of the reported analyses, even in the presence of more than 4000 nonlinear interface elements, remains comparable to that of a simple linear elastic one, a fact confirming the effectiveness of the proposed approach. On the other hand, we expect that a nonlinear analysis, performed on a 3-D mesh in which the PDL is described in terms of continuum, solid elements, such as done (on a much smaller model that includes a single tooth only) by Natali et al. [13], would have required a computational cost about one order of magnitude greater than that required by the analysis with the interface elements.

5 Discussion and Conclusions

A phenomenological approach to the analysis of the tooth/bone system has been proposed, making use of a nonlinear interface model of the PDL. The interface approach precludes the *direct* possibility of obtaining details of the stress and strain states *within* the PDL itself, but provides a reasonably simple and effective description of the *global* behavior of the system. On the other

hand, a stress analysis inside the PDL would be possible by means of a *postprocessing* of the results obtained with our model, when a micromechanical model of the PDL were available. The latter should take into account the complexity of the geometrical/mechanical properties of the internal structure of the PDL. Anisotropy due to fiber orientation, fluid-solid interaction, irreversibility, and time dependent response are all features clearly emerging from the experiments reported in [8]; unfortunately, such experiments are insufficient, both quantitatively and qualitatively, to allow us to formulate a reasonably accurate micromechanical model for the PDL. The coupling of the global analysis proposed in this article with a local micromechanical approach would avoid the complexity of a single, multiple-scale computation, so that the problem would be split into two simpler sub-tasks, without loss of accuracy.

Two main conclusions can be drawn from the present study:

- the description of the nonlinear behavior of the PDL produces extremely important effects on the computed mechanical quantities in a numerical model of the tooth-bone system;
- there is a clear theoretical and computational advantage in employing an interface model in the numerical analyses, rather than a continuum, three-dimensional one.

As stressed at the beginning of Section 4 (not fully illustrated for the sake of brevity), and as already pointed out by one of the Authors elsewhere [20], the use of a three-dimensional geometry is mandatory; plane models result definitely inadequate and should never be used to simulate the tooth/bone system under load.

The results obtained in the present paper suggest that the modeling of the PDL by means of interface elements, together with a detailed geometrical description of the jaw, should provide stress values accurate enough to be useful both to investigate related phenomena—such as bone remodeling, an analysis requiring a description of several complex phenomena, not addressed here—and as a starting point for the design of “optimal” implants, causing in the surrounding bone, upon loading, stress and strain states closely resembling those occurring around a healthy tooth. The reported results, however, should be considered only as a first step towards a precise mechanical characterization of the tooth-PDL-bone system. Indeed, several difficulties still need to be overcome. These are related to:

- the irreversibility of the PDL behavior, dominated by the presence and motion of the fluid phase, governed by its saturation index;
- the fiber contents of PDL, as well as the position, orientation, geometry, and stiffness of the fibers.

Work is currently in progress both to obtain better experimental results (on pig PDL, expected to be more similar to the human one than the bovine PDL tested in [8]), and to develop a suitable micromechanical model of the PDL [24], taking into account both the presence of the fibers and that of a fluid phase.

Finally, we remark that the proposed formulation of the interface constitutive law could also be applied to a version of the Boundary Element technique, allowing for “zones” of different elastic materials, connected by nonlinear interfaces. This approach is under current investigation (preliminary results to be found in Salvadori [25]).

Acknowledgments

The present work was performed within the research project “Criteri di progetto per impianti dentali ottimizzati rispetto alla stabilità biomeccanica dell’interfaccia osso-impianto” financed by the Italian Ministry of Education, University, and Research (MIUR). The Finite Element code ABAQUS has been run at the Department of Civil Engineering, University of Brescia, Italy, under an academic license. Thanks are due to Professors C. Pagan-

elli, S. Salgarello and P. L. Sapelli, of the Odontoiatric Clinic of the University of Brescia, Italy, for many helpful discussions, as well as to Drs. P. Fogazzi, P. Manfredini, and A. Redona, for their help with the numerical part of the work.

Appendix—Uniqueness of the Finite and the Incremental Problems

With reference to the tooth-PDL-bone system, let the bodies Ω^A and Ω^B represent the tooth and bone, respectively.

Suppose now that two solutions of the equilibrium problem for the system exist, such that the compatibility requirements on the displacements, and equilibrium for the forces, are satisfied. Let us denote these two solutions with $[\mathbf{u}^1, \boldsymbol{\varepsilon}^1, \boldsymbol{\sigma}^1, \mathbf{p}^1, \boldsymbol{\delta}^1]$ and $[\mathbf{u}^2, \boldsymbol{\varepsilon}^2, \boldsymbol{\sigma}^2, \mathbf{p}^2, \boldsymbol{\delta}^2]$, where $\boldsymbol{\varepsilon}$ is the infinitesimal strain tensor and \mathbf{p} is the traction exerted by the interface on the bone, i.e., $\mathbf{p} = \boldsymbol{\sigma}^B \mathbf{n}^B$ in $\Xi \in \partial\Omega^B$. In particular, under the assumption (25)

$$\mathbf{p} = S_m [f_n(\beta) \mathbf{n}^B + f_t(\gamma) \mathbf{t}^B]. \quad (26)$$

If we denote the difference between the two solutions by $\Delta(\cdot) = (\cdot)^1 - (\cdot)^2$, the application of the principle of virtual work yields

$$\int_{\Omega^A \cup \Omega^B} \Delta \boldsymbol{\sigma} \cdot \Delta \boldsymbol{\varepsilon} dV + \int_{\Xi} \Delta \boldsymbol{\delta} \cdot \Delta \mathbf{p} dA = 0. \quad (27)$$

For linear elastic materials, such as, by assumption, those defining regions Ω^A and Ω^B , governed by the constitutive fourth-order tensors \mathbb{E}^A and \mathbb{E}^B respectively, the quantities

$$\Delta \boldsymbol{\sigma} \cdot \Delta \boldsymbol{\varepsilon} = \Delta \boldsymbol{\varepsilon} \cdot \mathbb{E}^A \Delta \boldsymbol{\varepsilon}, \text{ in } \Omega^A, \quad \Delta \boldsymbol{\sigma} \cdot \Delta \boldsymbol{\varepsilon} = \Delta \boldsymbol{\varepsilon} \cdot \mathbb{E}^B \Delta \boldsymbol{\varepsilon}, \text{ in } \Omega^B, \quad (28)$$

are positive, and null if and only if $\Delta \boldsymbol{\varepsilon} = \mathbf{0}$. For this reason, the first integral in (27) is positive, and null only when $\Delta \boldsymbol{\varepsilon} = \mathbf{0}$. The terms appearing in the integrand of the second integral in (27) can be expanded as

$$\begin{aligned} \Delta \boldsymbol{\delta} &= \Delta \delta_n \mathbf{n}^B + \Delta \boldsymbol{\delta}_t, \\ \Delta \mathbf{p} &= S_m \left\{ f_n \left(\frac{\delta_n^1}{w_0} \right) - f_n \left(\frac{\delta_n^2}{w_0} \right) \right\} \mathbf{n}^B + S_m \left\{ f_t \left(\frac{\delta_t^1}{w_0} \right) \mathbf{t}_1^B - f_t \left(\frac{\delta_t^2}{w_0} \right) \mathbf{t}_2^B \right\}, \end{aligned} \quad (29)$$

so that

$$\begin{aligned} \Delta \boldsymbol{\delta} \cdot \Delta \mathbf{p} &= S_m \left\{ f_n \left(\frac{\delta_n^1}{w_0} \right) - f_n \left(\frac{\delta_n^2}{w_0} \right) \right\} \Delta \delta_n + S_m \left\{ f_t \left(\frac{\delta_t^1}{w_0} \right) \mathbf{t}_1^B \right. \\ &\quad \left. - f_t \left(\frac{\delta_t^2}{w_0} \right) \mathbf{t}_2^B \right\} \cdot \Delta \boldsymbol{\delta}_t. \end{aligned} \quad (30)$$

Each of the two terms on the right-hand side of (30) can be negative, owing to the decreasing part of functions f_n and f_t after the maximum. Therefore, Eq. (27) may be satisfied and the solution of the problem may be non-unique.

Uniqueness of solution of the incremental problem involves the incremental form of the principle of virtual work (27), namely

$$\int_{\Omega^A \cup \Omega^B} \Delta \dot{\boldsymbol{\sigma}} \cdot \Delta \dot{\boldsymbol{\varepsilon}} dV + \int_{\Xi} \Delta \dot{\boldsymbol{\delta}} \cdot \Delta \dot{\mathbf{p}} dA = 0, \quad (31)$$

where a superimposed dot indicates rate (incremental) quantities. Taking now the rates of (29), we obtain

$$\begin{aligned} \Delta \dot{\boldsymbol{\delta}} &= \Delta \dot{\delta}_n \mathbf{n}^B + \Delta \dot{\boldsymbol{\delta}}_t + \delta_t \Delta \dot{\mathbf{t}}^B, \\ \Delta \dot{\mathbf{p}} &= S_m \left(\frac{df_n}{d\delta_n} \Delta \dot{\delta}_n \right) \mathbf{n}^B + S_m \left(\frac{df_t}{d\delta_t} \Delta \dot{\delta}_t \right) \mathbf{t}^B + S_m f_t \Delta \dot{\mathbf{t}}^B, \end{aligned} \quad (32)$$

so that the rate analogous of (30) is

$$\Delta \dot{\boldsymbol{\delta}} \cdot \Delta \dot{\mathbf{p}} = S_m \frac{df_n}{d\delta_n} (\Delta \dot{\delta}_n)^2 + S_m \frac{df_t}{d\delta_t} (\Delta \dot{\delta}_t)^2 + S_m \delta_t f_t |\Delta \dot{\mathbf{t}}^B|^2, \quad (33)$$

where we have used the orthogonality condition $\mathbf{t}^B \cdot \Delta \dot{\mathbf{t}}^B = 0$, following from the fact that \mathbf{t}^B is a unit vector. From (33), observing that $S_m \delta_t f_t |\Delta \dot{\mathbf{t}}^B|^2$ is always non-negative, we may conclude that a solution of the incremental problem is necessarily unique when both incremental stiffnesses $df_n/d\delta_n$ and $df_t/d\delta_t$ are strictly positive.

References

- [1] McGuinness, N. J. P., Wilson, A. N., Jones, M. L., and Middleton, J., 1991, "A Stress Analysis of the Periodontal Ligament Under Various Orthodontic Loadings," *European Journal of Orthodontics*, **13**, pp. 231–242.
- [2] Middleton, J., Jones, M. L., and Wilson, A. N., 1996, "The Role of the Periodontal Ligament in Bone Modeling: The Initial Development of a Time-Dependent Finite Element Model," *Am. J. Orthod. Dentofacial Orthop.*, **109**, pp. 155–162.
- [3] Rees, J. S., and Jacobsen, P. H., 1997, "Elastic Modulus of the Periodontal Ligament," *Biomaterials*, **18**, pp. 995–999.
- [4] Moxham, B. J., and Berkovitz, B. K. B., 1982, "The Effects of External Forces on the Periodontal Ligament—The Response to Axial Loads," in *The Periodontal Ligament in Health and Disease*, B. K. B. Berkovitz, B. J. Moxham, and H. W. Newman, eds., Pergamon Press, Oxford, pp. 249–268.
- [5] van Rossen, I. P., Braak, L. H., de Putter, C., and de Groot, K., 1990, "Stress-Absorbing Elements in Dental Implants," *J. Prosthet. Dent.*, **64**(2), pp. 198–205.
- [6] Brunski, J. B., 1992, "Biomechanical Factors Affecting the Bone-Dental Implant Interface," *Clinical Materials*, **10**, pp. 153–201.
- [7] Ralph, W. J., 1982, "Tensile Behavior of the Periodontal Ligament," *Journal of Periodontal Research*, **17**, p. 423–426.
- [8] Pini, M., 1999, "Mechanical Characterization and Modeling of the Periodontal Ligament," PhD thesis, University of Trento, Trento, Italy.
- [9] Pini, M., Vena, P., and Contro, R., 2000, "Parameter Identification of a Non-Linear Constitutive Law for the Periodontal Ligament Allowing for Tensile and Shear Laboratory Tests," *Proc. XIII Convegno Italiano di Meccanica Computazionale*, Brescia, Italy, 13–15 November 2000.
- [10] Fung, Y. C., 1993, *Biomechanics: Mechanical Properties of Living Tissues*, Springer-Verlag, Berlin, Heidelberg.
- [11] Pietrzak, G., 1997, "Continuum Mechanics Modeling and Augmented Lagrangian Formulation of Large Deformation Frictional Contact Problems," PhD thesis, LMAF-DGM-EPFL, Lausanne, Switzerland.
- [12] Pietrzak, G., Botsis, J., Curnier, A., Zysset, P., Scherrer, S., Wiskott, A., and Belsler, U., 1998, "Numerical Identification of Material Properties of the Periodontal Ligament," *Societe de Biomecanique, Actes du 23eme Congres*, INSA, Lyon, France, p. 203.
- [13] Natali, A., Pavan, P., Pini, M., and Ronchi, R., 2000, "Numerical Analysis of Short Time Response of Periodontal Ligament," *Proc. 12th Conference of the European Society of Biomechanics*, Dublin, Ireland.
- [14] Goland, M., and Reissner, E., 1944, "The Stresses in Cemented Joints," *J. Appl. Mech.*, **11**, pp. A17–A27.
- [15] Jones, J. P., and Whittier, J. S., 1967, "Waves at a Flexibly Bonded Interface," *ASME Trans. J. Appl. Mech.*, **34**, pp. 905–909.
- [16] Klarbring, A., 1991, "Derivation of a Model of Adhesively Bonded Joints by the Asymptotic Expansion Method," *Int. J. Eng. Sci.*, **29**, pp. 493–512.
- [17] Truesdell, C. A., and Noll, W., 1965, "The Non-Linear Field Theories of Mechanics," in *Handbuch der Physik*, S. Flügge, ed., Vol. III/3, Springer-Verlag, Berlin.
- [18] Needleman, A., 1990, "An Analysis of Tensile Decohesion Along an Interface," *J. Mech. Phys. Solids*, **38**, pp. 289–324.
- [19] Hibbit, Karlsson & Sorensen, 2001, "ABAQUS User's Manuals," Release 6.2, Pawtucket, RI, USA.
- [20] Corradi, L., and Genna, F., 2002, "Finite Element Analysis of the Jaw-Teeth/Dental Implant System: A Note About Geometrical and Material Modeling," *Computer Modeling in Engineering and Sciences*, to appear.
- [21] Goodman, R. E., Taylor, R. L., and Brekke, T. L. 1968, "A Model for the Mechanics of Jointed Rock," *Journal of Soil Mechanics and Foundation Division, Proceedings of the ASCE*, **94**, pp. 637–659.
- [22] Meijer, H. J. A., Starman, F. J. M., Steen, W. H. A., and Bosman, F., 1993, "A Three-Dimensional, Finite-Element Analysis of Bone Around Dental Implants in an Edentulous Human Mandible," *Arch. Oral Biol.*, **38**, pp. 491–496.
- [23] Jäger, K., and Dietrich, H., 1991, "Measuring Masticatory Forces with Strain Gages," *RAM*, **7**, pp. 39–42.
- [24] Perelmuter, M. N., 2001, "Development of a Micromechanically Based Interface Law for the Periodontal Ligament," Internal Report, Landau Network-Centro Volta Fellowship, Department of Civil Engineering, University of Brescia, Italy.
- [25] Salvadori, A., 2000, "Symmetric Galerkin BEM for Domains Connected by Cohesive Interfaces: Formulation and Implementation," *Proc. XIII Convegno Italiano di Meccanica Computazionale*, Brescia, Italy, 13–15 November 2000.